ARMY RESEARCH LABORATORY

Notch Dimensions for Three-Point Bend Fracture Specimens Based On Compliance Analyses

Francis I. Baratta and
John H. Underwood

ARL-TR-35

December 1992

The findings in this report are not to be construed as an official Department of the Army position, unless so designated by other authorized documents.

Mention of any trade names or manufacturers in this report shall not be construed as advertising nor as an official indorsement or approval of such products or companies by the United States Government.

DISPOSITION INSTRUCTIONS

Destroy this report when it is no longer needed.
Do not return it to the originator

REPORT DOCUMENTATION PAGE

Form Approved
OMB No. 0704-0188

1. AGENCY USE ONLY *(Leave blank)*	2. REPORT DATE	3. REPORT TYPE AND DATES COVERED
	December 1992	Reprint - Final Report

4. TITLE AND SUBTITLE
NOTCH DIMENSIONS FOR THREE-POINT BEND FRACTURE SPECIMENS BASED ON COMPLIANCE ANALYSES

5. FUNDING NUMBERS

6. AUTHOR(S)
Francis I. Baratta and John H. Underwood*

7. PERFORMING ORGANIZATION NAME(S) AND ADDRESS(ES)
U.S. Army Research Laboratory
Watertown, Massachusetts 02172-0001
ATTN: AMSRL-MA-CA

8. PERFORMING ORGANIZATION REPORT NUMBER
ARL-TR-35

9. SPONSORING/MONITORING AGENCY NAME(S) AND ADDRESS(ES)
U.S. Army Research Laboratory
2800 Powder Mill Road
Adelphi, Maryland 20783-1197

10. SPONSORING/MONITORING AGENCY REPORT NUMBER

11. SUPPLEMENTARY NOTES
Published in Journal of Testing and Evaluation, JTEVA, v. 20, no. 5, September 1992, pp. 343-348.

12a. DISTRIBUTION/AVAILABILITY STATEMENT
Approved for public release; distribution unlimited.

12b. DISTRIBUTION CODE
A

13. ABSTRACT *(Maximum 200 words)*
Load-line compliance was calculated for various three-point bend specimens containing finite width notches and cutouts, using methods of engineering strength of materials and elastic superposition. Comparison of compliance results for notched specimens with results for the ideal zero width crack was used to propose two basic notch configurations for fracture testing. A relatively wide notch that could be produced by conventional manufacturing methods resulted in load-line compliance values 10% or more above those of the ideal crack case. A narrow notch that could be produced by electric-discharge machining resulted in compliance values much closer to those of the ideal crack case.

14. SUBJECT TERMS
Fracture toughness, Compliance, Strength of materials, Bending beam, and Notch analysis

15. NUMBER OF PAGES
9

16. PRICE CODE

17. SECURITY CLASSIFICATION OF REPORT	18. SECURITY CLASSIFICATION OF THIS PAGE	17. SECURITY CLASSIFICATION OF ABSTRACT	20. LIMITATION OF ABSTRACT
Unclassified	Unclassified	Unclassified	UL

Francis I. Baratta[1] *and John H. Underwood*[2]

Notch Dimensions for Three-Point Bend Fracture Specimens Based on Compliance Analyses

REFERENCE: Baratta, F. I. and Underwood, J. H., "**Notch Dimensions for Three-Point Bend Fracture Specimens Based on Compliance Analyses.**" *Journal of Testing and Evaluation*, JTEVA, Vol. 20, No. 5, Sept. 1992, pp. 343–348.

ABSTRACT: Load-line compliance was calculated for various three-point bend specimens containing finite width notches and cutouts, using methods of engineering strength of materials and elastic superposition. Comparison of compliance results for notched specimens with results for the ideal zero width crack was used to propose two basic notch configurations for fracture testing. A relatively wide notch that could be produced by conventional manufacturing methods resulted in load-line compliance values 10% or more above those of the ideal crack case. A narrow notch that could be produced by electric-discharge machining resulted in compliance values much closer to those of the ideal crack case.

KEY WORDS: fracture toughness, compliance, strength of materials, bending beam, notch analysis

Nomenclature

- a Total length of crack plus notch (Figs. 1–3)
- a_F Extension of notch by fatigue crack (Figs. 1–3)
- a_N Notch dimension (Figs. 1–3)
- B Specimen thickness (Figs. 1–3)
- b, b_c Specimen dimensions (Figs. 1–3)
- E, E' Elastic modulus; (E' for plane strain)
- H Notch dimension ($L - a_N$)
- L Notch length (Figs. 1–3)
- L_c, N_c Cutout dimensions (Figs. 1–3)
- N Notch width (Figs. 1–3)
- P Applied load (Figs. 1–3)
- U_a, U_b Elastic strain energy; case a and b (Fig. 3)
- S Specimen span (Figs. 1–3)
- W Specimen depth (Figs. 1–3)
- α Normalized total length of notch plus crack (a/W)
- α_N Normalized notch dimension (a_N/W)
- β Crack envelope angle (Figs. 1–3)
- γ Included notch-tip angle (Figs. 1–3)
- δ Load-line displacement of beam (Figs. 1–3)
- Ω Normalized notch dimension (H/W)
- Ω_c Normalized notch dimension (L_c/W)
- Δ Normalized load-line compliance ($\delta EB/P$)
- Δ_c Normalized load-line compliance due to cutout ($\delta_c EB/P$)
- Δ_{ideal} Normalized load-line compliance due to an ideal zero-width crack ($\delta EB/P$)
- μ Poisson's ratio

Manuscript received 2/28/91; accepted for publication 2/7/92.

[1]Research Engineer, Army Materials Technology Laboratory, Watertown, MA.

[2]Research Engineer, Army Armament Research, Development and Engineering Center, Watervliet, NY.

Introduction

Technical committees within ASTM Committee E24 on Fracture are currently developing a comprehensive fracture toughness test method that will include many of the procedures of existing fracture testing standards. The intent is to provide a "common" fracture toughness test method that could be used for any of four basic types of fracture behavior that are currently investigated using the following methods: E399 for Plain-Strain Fracture Toughness of Metallic Materials; E813 for J_{Ic}, A Measure of Fracture Toughness; E1152 for Determining J-R Curves; and E1290 for Crack-Tip Opening Displacement (CTOD) Fracture Toughness Measurement.

The specimen configuration included in each of the four test methods is the three-point bend specimen. Two of the methods, E813 and E1152, require load-line compliance determination by both experimental means and theoretical analysis. These test methods refer to a formulation of load-line compliance based on results of the authors [*1*]. In this work, any given combination of machined notch plus crack extension was represented as an ideal zero-width crack, and the effect of the finite width notch on the beam compliance was ignored. The compliance contributed by the finite width of the notch, although not the major contributor to compliance, can be substantial, depending on the notch and crack dimensions. In many cases this additional compliance attributable to the notch width can be ignored; but if accurate load-line compliance results are desired, the notch configuration should be considered in the analysis. Baratta [*2*] recently provided relevant results, wherein he determined that in some instances errors resulting from the use of Ref *1* as applied to fracture testing were considerable.

Considering the above, the objective here is to use the method and results of Baratta [*2*] to (1) calculate load-line compliance for various notch and crack configurations, and (2) provide guidance to ASTM technical committees in defining appropriate and practical geometry limits to minimize load-line compliance errors in fracture testing with three-point bend specimens.

Analysis

Little detail is given here of the method for obtaining load-line compliance of a three-point bend beam because it is well documented in the literature [2]. However, some general comments are appropriate.

A simple, yet accurate, way of calculating compliance for stepped structural elements has been provided by Bluhm [3]. Engineering strength of materials analysis was combined with elastic fracture mechanics to obtain deflections of geometrically discontinuous structures. The method was based on the work of Paris [4] and subsequently Tada et al. [5], where techniques for computing certain displacements in crack-related problems were suggested. Bluhm's approach as applied to stepped structures was adapted by Baratta to various V-notched configurations using superposition. Specifically, the configuration examined by Baratta, and also appropriate to the topic here, is shown in Fig. 1. For this three-point bend specimen with $S/W = 4$, and using the methods outlined above, the normalized load-line compliance including the effects of notch configuration, taken from reference 2, is[3]:

$$\Delta = [(b/W)^3/4] + [[3(1+\mu)/5][b/W - 2\tan(\gamma/2)\ln(1 - \alpha_N/\{1-\Omega\})]] + [3\tan(\gamma/2)][[S/(2W\{1-\Omega-\alpha_N\})]^2 - [b/(2W\{1-\Omega\})]^2 - [2\tan(\gamma/2)][S/(2W\{1-\Omega-\alpha_N\}) - b/(2W\{1-\Omega\}) + \tan(\gamma/2)\ln(1-\alpha_N/\{1-\Omega\})]] + [f(\alpha)] \quad (1)$$

where from the work of Wu Shang-Xian [6]:

$$f(\alpha) = 18(S/2W)^2[-0.365\alpha^5 + 1.326\alpha^4 - 2.71\alpha^3 + 3.87\alpha^2 - 8.614\alpha - 2.268 + 6.018\ln(1+2\alpha) - 1.015\ln(1-\alpha) + (2.829\alpha^2 - 4.437\alpha + 2.268)/\{(1+2\alpha)(1-\alpha)^2\}] \quad (2)$$

Equation 1 applies to a plane stress condition; simply multiply $f(\alpha)$ by the quantity $(1 - \mu^2)$, and the plain strain condition is realized. Equation 1 does not account for the compliance due to the radius at the apex of the V-notch nor for the local discontinuities at the junction of the V-notch and the straight sides of the notch. However, it is expected that the effect of these subtle geometric details of the notch on the load-line compliance will be negligible.

Equation 1 also does not account for a displacement gage cutout, such as that shown in Fig. 2. The displacement and associated compliance due to the cutout can be readily accounted for by superposition of the two cases shown in Fig. 3. This has been accomplished, see the Appendix, resulting in an additional normalized compliance, Δ_c, given by:

$$\Delta_c = 3[\{(b/2W)^2 - (b_c/2W)^2\}/\{1-\Omega_c\}^2 - 2(b/2W - b_c/2W)(\{1+\mu\}/5 + 1/\{1-\Omega_c\})] \quad (3)$$

[3]Note that this equation in reference 2 has a typographical error; Eq 1 above is correct.

The total load-line compliance, Δ_T, is simply the sum of Eqs 1 and 3:

$$\Delta_T = \Delta + \Delta_c \quad (4)$$

In the results to follow, load-line compliance for various notched configurations are presented and compared with the ideal crack results [1]. The expression for load-line compliance for the case of an ideal crack, Δ_{ideal}, from reference 1, is the following:

$$\Delta_{ideal} = [(S/W)/(1-\alpha)]^2[1.193 - 1.980\alpha + 4.478\alpha^2 - 4.443\alpha^3 + 1.739\alpha^4] \quad (5)$$

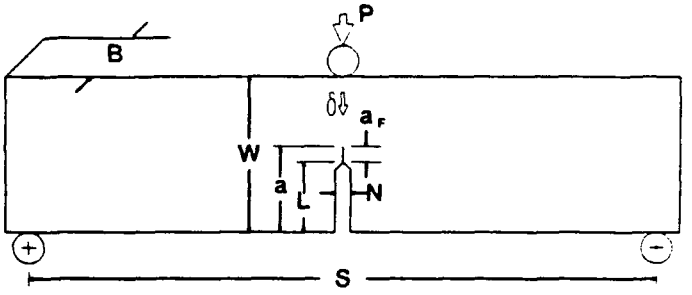

FIG. 1—*Three-point bend specimen configuration.*

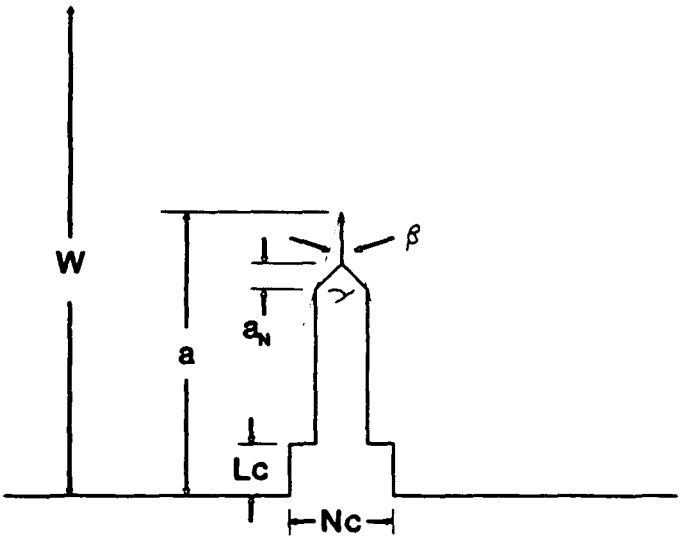

FIG. 2—*Notch and cutout configuration.*

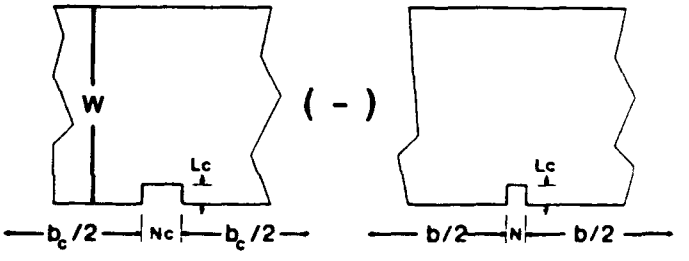

FIG. 3—*Cutout configurations for superposition.*

Results

Notch and cutout configurations were selected to show what were believed to be the key factors which affect load-line compliance and also to show the more significant differences in compliance for the finite-thickness notch and the ideal crack, Eqs 4 and 5, respectively. The range of configurations selected covered those of interest in the fracture test methods mentioned earlier. Figures 4 through 7 and Tables 1 and 2 show the results.

Figure 4 compares the normalized load-line compliance, $\Delta = \delta EB/P$, for the ideal zero-width crack (Eq 5) with results for notches of various widths (Eq 4), over a range of a/W. Note that the increase in compliance due to the finite width of the notch becomes more significant for deeper notches. The relative change in compliance, compared to that for an ideal crack, can be more directly considered when plotted as a ratio, Δ/Δ_{ideal}, see Fig. 5. These results can be used to show the upper bound differences in compliance between three-point bend specimens with a finite thickness notch and specimens with an idealized crack, for a variety of notch and crack lengths. For example, consider a beam having a notch length, $L = 0.425\ W$ (the lower curve) and a fatigue crack length of $a_F = 0.025\ W$ (the smallest fatigue crack considered here) giving a total notch-plus-crack length of $a = 0.45\ W$. For this configuration the difference in compliance from that of the idealized crack is 7.3%. However, as a_F is allowed to increase this difference is reduced, to a value of 2.0% when $a_F = 0.325\ W$ and $a = 0.75\ W$. Thus, it is seen that a large notch depth with a small fatigue crack produces a significant increase in compliance over that of the ideal crack. The end points of the family of curves for a range of L/W values produce an upper bound description of the increase in compliance, the dashed line in Fig. 5. For most real testing situations the difference in compliance will be less than these maximum values, because $a_F > 0.025\ W$.

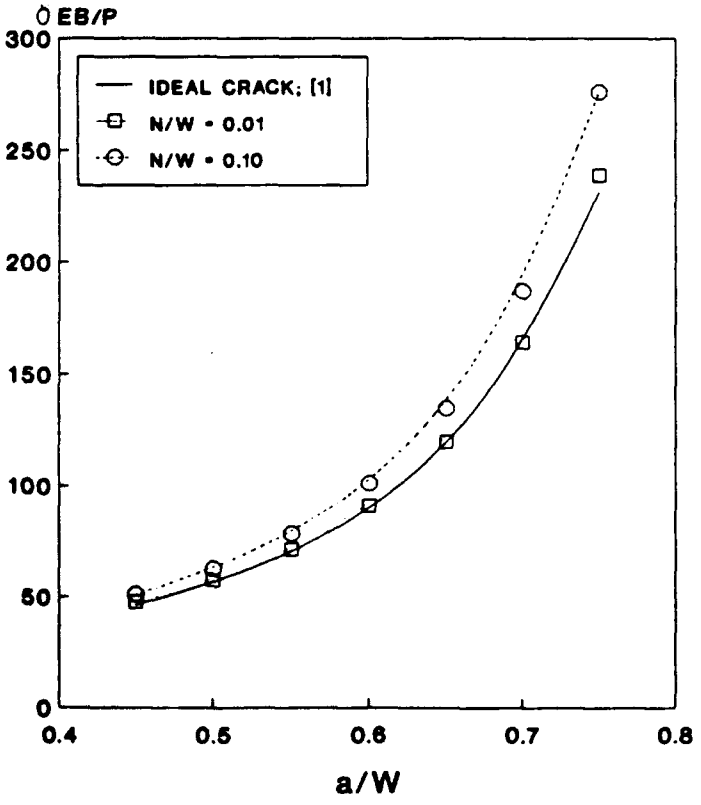

FIG. 4—*Comparison of normalized load-line compliance for three-point bend specimens with notches and ideal crack; notched configurations are:* $\gamma = 90°$, $a_F/W = 0.025$, $N_c/W = 0.2$, $L_c/W = 0.1$.

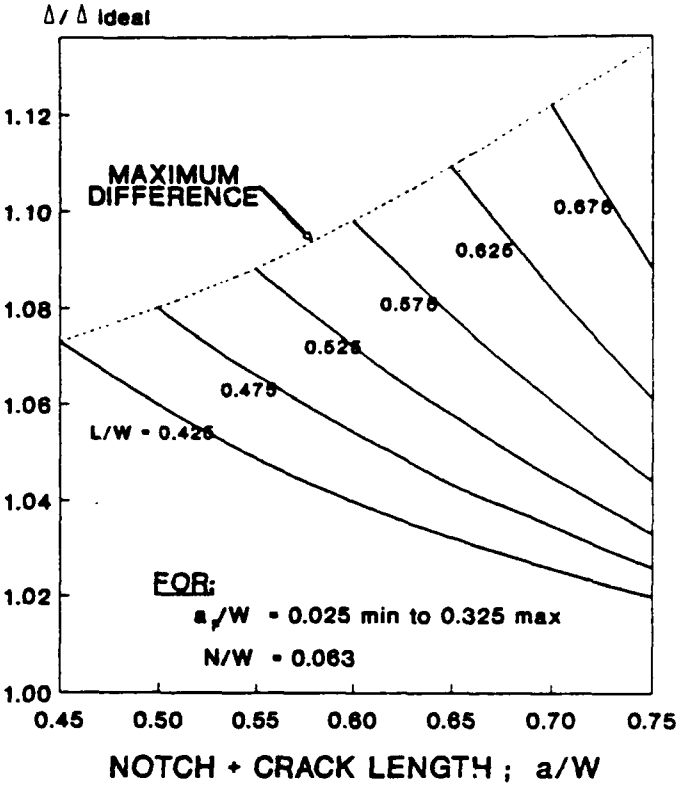

FIG. 5—*Compliance differences for three-point bend specimens with various lengths of idealized crack and notch plus crack; notched configurations are:* $\gamma = 90°$, $N_c/W = 0.2$, $L_c/W = 0.1$.

Figures 6 and 7 show the effect on compliance of important configurational variables. Figure 6 shows the Δ/Δ_{ideal} values for three finite notch widths (solid lines with symbols) compared with the ideal crack, with $\Delta/\Delta_{ideal} = 1$ (the solid line). The notches each have $a_F/W = 0.025$ and $\gamma = 90°$. Note the significant effect on compliance due to notch width, with a value of $N/W = 0.10$ resulting in a 10–19% increase over that of the ideal crack, for the range $0.45 \le a/W \le 0.75$. The lesser effect of two other configurational features on compliance can also be seen. The amount of crack extension from the notch tip, a_F/W, has less affect on compliance than notch width; note that the dashed curve for $a_F/W = 0.050$ is reduced as would be expected (the additional crack extension makes the notch behave a bit more like an ideal crack), but the reduction is only about 2%. The effect of the cutout on compliance can be judged from the dotted curve. The cutout with $L_c/W = 0.1$ and $N_c/W = 0.2$ adds only about 1% to compliance for $a/W = 0.45$, and its addition diminishes as a/W increases.

The effect of notch-tip included angle, γ, on compliance is considered in Fig. 7. It can be seen that if γ were 30° rather than 90° about one third of the compliance increase due to the notch would be eliminated, for this notch ($N/W = 0.10$; $a_F/W = 0.025$). However, the fabrication difficulties associated with a 30° notch-tip angle would be significant for many users. In addition, the

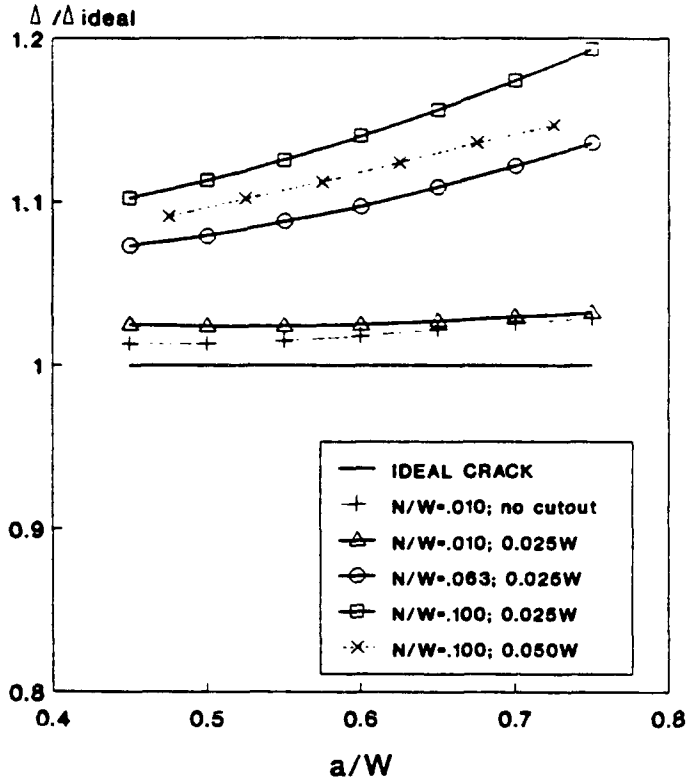

FIG. 6—*Effects of notch width* (N), *cutout dimensions* (N_c, L_c) *and crack extension* (a_F) *on load-line compliance for three-point bend specimens; notched configurations are:* $\gamma = 90°$, $N_c/W = 0.2$, $L_c/W = 0.1$.

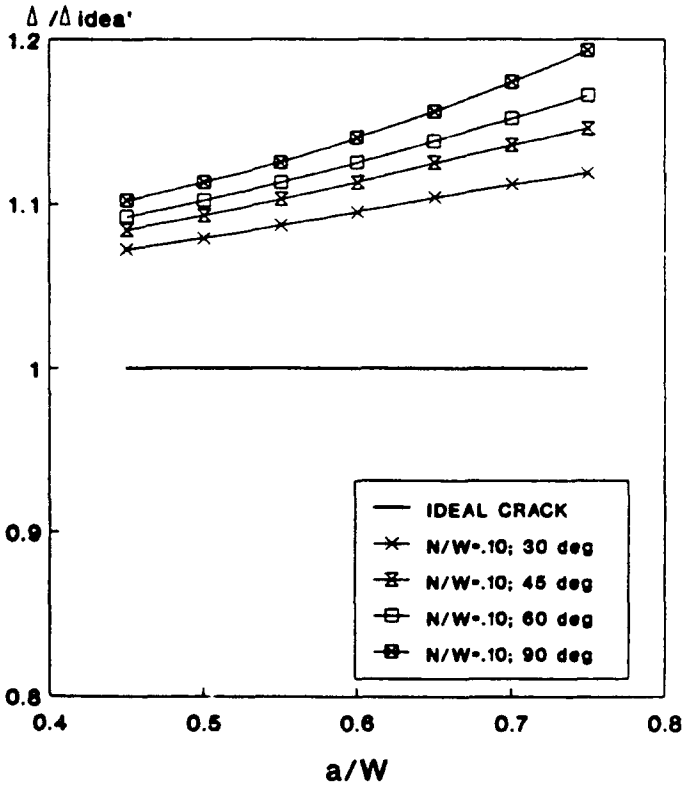

FIG. 7—*Effect of notch-tip angle* (α) *on load-line compliance for three-point bend specimens; notched configurations are:* $a_F/W = 0.025$, $N_c/W = 0.2$, $L_c/W = 0.1$.

effect of a small γ in eliminating some of the compliance increase due to the notch will be greatly diminished for notches with smaller N/W and larger a_F/W.

Values of normalized compliance for various notch and crack configurations, including many of those of Figs. 4 through 7, are listed in Tables 1 and 2. Also shown are the values of the crack and notch envelope angle, β, for each configuration, see Fig. 2. Historically, a limitation on this envelope angle has been used to insure that a given notch configuration is a reasonable simulation of an ideal crack (see Appendix). Although a general trend can be noted in Table 1, in which a small envelope angle is associated with a small difference between notch and ideal crack compliance, the trends already described between notch dimensions and compliance are better defined.

Discussion

The results of solid mechanics analyses described here were used to suggest two sets of notch and cutout dimensions for use in fracture tests with the three-point bend specimen. We believe that these same dimensions are also applicable to other configurations which are subjected to predominantly bending stresses, including the compact specimen used in many fracture tests and the arc and disk shaped specimens used in ASTM Method E399. In addition to analytical results, some engineering experience and judgment were used in arriving at the suggested specimen dimensions, particularly as related to specimen fabrication and test procedures in common use today.

Table 3 gives the two suggested notch and cutout configurations, as a list of five required dimensions: the maximum allowed notch width, N/W; the maximum allowed notch-tip included angle, γ; the minimum required crack extension, a_F/W; the maximum allowed cutout length and width, L_c and N_c. The current requirements in ASTM Methods E399 and E813 are listed for reference.

The most significant change in specimen configuration involves notch width, where a wide notch with $N/W = 0.063$ is suggested for tests in which specimen fabrication requirements are controlling, and a narrow notch with $N/W = 0.01$ is suggested for tests in which a close modeling of the ideal crack compliance is important. The wide notch can be easily cut in relatively large specimens using conventional machining, whereas the narrow notch requires a quite narrow slitting process, such as electric-discharge machining. The other notch and crack dimensions are unchanged from existing methods. Although some narrowing of the difference in compliance of the real notch and cutout compared to the ideal crack could have been accomplished with tighter dimensions, the user would have paid dearly in fabrication and testing difficulties.

The final result of the suggested notch, crack and cutout dimensions is: (1) for the wide notch the compliance can be 7 to 12% above that of the ideal crack, for $0.45 \leq a/W \leq 0.75$, respectively; (2) for the narrow notch the compliance is 3% above that of the ideal crack, for the range $0.45 \leq a/W \leq 0.75$. It should be noted that generally only the lower end of the possible 7 to 12% increase in compliance mentioned above would be experienced in fracture testing because, although R-curve type tests are often performed for $a/W \approx 0.7$, the notch length is generally at $a/W \approx 0.6$ or less.

TABLE 1—*Load-line compliance for three-point bend specimens with various notch widths and crack configurations.*

Notch Width, N/W	Cutout Dimensions L_c/W	Cutout Dimensions N_c/W	Tip Angle, γ deg	Crack Extension, a_f/W	Envelope Angle, β deg	Notch + Crack Length, a/W	Normalized Compliance, $\delta EB/P$
0.100	0.10	0.20	90	0.050	53.1	0.475	55.49
						0.525	68.51
						0.575	86.75
						0.625	113.20
						0.675	153.34
						0.725	218.03
0.063	0.10	0.20	90	0.025	58.1	0.45	49.67
						0.50	60.51
						0.55	75.49
						0.60	96.88
						0.65	128.65
						0.70	178.44
						0.75	262.43
0.010	0.10	0.20	90	0.025	18.9	0.45	47.46
						0.50	57.39
						0.55	71.07
						0.60	90.49
						0.65	119.16
						0.70	163.77
						0.75	238.42
0.010	0.0 (No Cutout)	0.0	90	0.025	18.9	0.45	46.87
						0.50	56.80
						0.55	70.48
						0.60	89.90
						0.65	118.57
						0.70	163.19
						0.75	237.83
0.0	(Ideal Crack; Eq. 5)					0.45	46.29
						0.50	56.05
						0.55	69.41
						0.60	88.28
						0.65	116.01
						0.70	159.08
						0.75	231.10

TABLE 2—*Load-line compliance for three-point bend specimens with various notch-tip included angles.*

Notch Width, N/W	Cutout Dimensions L_c/W	Cutout Dimensions N_c/W	Tip Angle, γ deg	Crack Extension, a_f/W	Envelope Angle, β deg	Notch + Crack Length, a/W	Normalized Compliance, $\delta EB/P$
0.100	0.10	0.20	30	0.025	26.6	0.45	49.63
						0.50	60.49
						0.55	75.45
						0.60	96.70
						0.65	128.09
						0.70	176.93
						0.75	258.52
0.100	0.10	0.20	45	0.025	37.9	0.45	50.20
						0.50	61.26
						0.55	76.54
						0.60	98.28
						0.65	130.48
						0.70	180.72
						0.75	264.92
0.100	0.10	0.20	60	0.025	48.3	0.45	50.55
						0.50	61.75
						0.55	77.24
						0.60	99.31
						0.65	132.07

(Continued on next page)

TABLE 2—*Continued.*

Notch Width, N/W	Cutout Dimensions L_c/W	Cutout Dimensions N_c/W	Tip Angle, γ deg	Crack Extension, a_F/W	Envelope Angle, β deg	Notch + Crack Length, a/W	Normalized Compliance, $\delta EB/P$
						0.70	183.30
						0.75	269.43
0.100	0.10	0.20	90	0.025	67.4	0.45	50.99
						0.50	62.37
						0.55	78.12
						0.60	100.64
						0.65	134.16
						0.70	186.78
						0.75	275.69

TABLE 3—*Suggested notch dimensions for three-point bend fracture specimens: see Figs. 1 and 2.*

		Existing Standards		Suggestions from Compliance	
		E399	E813	Wide Notch	Narrow Notch
Max width:	N	0.100W	0.063W	0.063W	0.010W
Max tip angle:	γ	90°	—	90°	90°
Min extension:	a_F	0.025W	0.050a	0.025W	0.025W
Max cutout:	L_c	—	0.10W	0.10W	0.10W
Max cutout:	N_c	—	0.20W	0.20W	0.20W

APPENDIX

Compliance Due to Cutout

The displacement due to an additional cutout, such as that shown in Fig. 2 to accommodate a displacement gage, is required to obtain the total displacement of the beam configuration. All that is needed is the superposition of the two cases shown in Fig. 3 This contribution is then added to the compliance given by Eq 1.

The increase in strain energy of a notched beam due to shear loading and beam bending can be obtained from reference 2, Eqs 40 and 42, respectively. With $\gamma = \pi$, $\alpha_v = 0$, and redefining $\Omega = \Omega_c = L_c/W$, we then have for case a, $b = b_c$ and for case b, $b = b$. Substitution of these values into the appropriate equations cited above and subtracting the strain energy due to case b from that due to case a results in

$$U_a - U_b = [3P^2/2BE][(b/(2W\{1 - \Omega_c\}))^2 - (b_c/(2W\{1 - \Omega_c\}))^2 - 2(b/(2W\{1 - \Omega_c\}) - b_c/(2W\{1 - \Omega_c\}))] - [3(1 + \mu)P^2(b/W - b_c/W)/(10BE)] \quad (6)$$

Since the displacement of the beam due to the cutout, δ_c, is

$$\delta_c = d/dP(U_a + U_b) \quad (7)$$

Then

$$\Delta_c = 3[(\{b/2W\}^2 - \{b_c/2W\}^2)/(1 - \Omega_c)^2 - 2(b/2W - b_c/2W)(\{1 + \mu\}/5 + 1/\{1 - \Omega_c\})] \quad (8)$$

which is added to Eq 1 to obtain the total compliance Δ_T.

Equation 8 accounts for the additional compliance due to a cutout. However, the compliance due to discontinuities at the corners of the cutout are ignored, but this should be small compared to that given by Eq 8.

Crack Envelope Angle

Historically, the crack envelope angle, β, shown in Fig. 2, has been used (see ASTM Methods E561 and E647) to insure that the fatigue crack extension to the notch is large enough such that the stress intensity factor (or compliance) is not overly influenced by the notch configuration. With the aid of Fig. 2 the envelope angle is readily defined in terms of the notch configuration as follows:

$$\beta = 2 \tan^{-1}[N/2(a_v + a_F)]$$

and since $a_v = N/2(\tan\{\gamma/2\})$, then

$$\beta = 2 \tan^{-1}[1/(1/\tan\{\gamma/2\} + 2a/N)] \quad (9)$$

References

[1] Underwood, J. H., Kapp, J. A., and Baratta, F. I., "More on Compliance of the Three-Point Bend Specimen," *International Journal of Fracture*, Vol. 28, 1985, pp. R41–R45.

[2] Baratta, F. I., "Load-Point Compliance of a Three-Point Loaded Cracked-Notched Beam," *Journal of Testing and Evaluation*, Vol. 16, 1988, pp. 59–71.

[3] Bluhm, J. I., "Application of Fracture Mechanics to the Calculation of Deflection in Stepped Structural Elements," *Mechanics of Crack Growth, STP 590*, American Society for Testing and Materials, Philadelphia, 1976, pp. 420–428.

[4] Paris, P. C., "The Mechanics of Fracture Propagation and Solution to Fracture Arrestor Problems," Document D-2-2195, The Boeing Co., Seattle, WA, 1957.

[5] Tada, H., Paris, P. C., and Irwin, G. R., "*The Stress Analysis of Cracks Handbook*," Del Research Corp., Hellertown, PA, 1973, p. B-1.

[6] Wu Shang-Xian, "Crack Length Calculation Formula for Three Point Bend Specimens," *International Journal of Fracture*, Vol. 24, 1984, pp. R33–R35.

DISTRIBUTION LIST

No. of Copies	To
1	Office of the Under Secretary of Defense for Research and Engineering, The Pentagon, Washington, DC 20301
	Director, U.S. Army Research Laboratory, 2800 Powder Mill Road, Adelphi, MD 20783-1197
1	ATTN: AMSRL-OP-CI-A
	Commander, Defense Technical Information Center, Cameron Station, Building 5, 5010 Duke Street, Alexandria, VA 22304-6145
1	ATTN: DTIC-FDAC
1	MIA/CINDAS, Purdue University, 2595 Yeager Road, West Lafayette, IN 47905
	Commander, Army Research Office, P.O. Box 12211, Research Triangle Park, NC 27709-2211
1	ATTN: Information Processing Office
	Commander, U.S. Army Materiel Command, 5001 Eisenhower Avenue, Alexandria, VA 22333
1	ATTN: AMCSCI
	Commander, U.S. Army Materiel Systems Analysis Activity, Aberdeen Proving Ground, MD 21005
1	ATTN: AMXSY-MP, H. Cohen
	Commander, U.S. Army Missile Command, Redstone Scientific Information Center, Redstone Arsenal, AL 35898-5241
1	ATTN: AMSMI-RD-CS-R/Doc
1	AMSMI-RLM
	Commander, U.S. Army Armament, Munitions and Chemical Command, Dover, NJ 07801
2	ATTN: Technical Library
	Commander, U.S. Army Natick Research, Development and Engineering Center, Natick, MA 01760-5010
1	ATTN: Technical Library
	Commander, U.S. Army Satellite Communications Agency, Fort Monmouth, NJ 07703
1	ATTN: Technical Document Center
	Commander, U.S. Army Tank-Automotive Command, Warren, MI 48397-5000
1	ATTN: AMSTA-ZSK
1	AMSTA-TSL, Technical Library
	Commander, White Sands Missile Range, NM 88002
1	ATTN: STEWS-WS-VT
	President, Airborne, Electronics and Special Warfare Board, Fort Bragg, NC 28307
1	ATTN: Library
	Director, U.S. Army Ballistic Research Laboratory, Aberdeen Proving Ground, MD 21005
1	ATTN: SLCBR-TSB-S (STINFO)
	Commander, Dugway Proving Ground, UT 84022
1	ATTN: Technical Library, Technical Information Division
	Commander, Harry Diamond Laboratories, 2800 Powder Mill Road, Adelphi, MD 20783
1	ATTN: Technical Information Office
	Director, Benet Weapons Laboratory, LCWSL, USA AMCCOM, Watervliet, NY 12189
1	ATTN: AMSMC-LCB-TL
1	AMSMC-LCB-R
1	AMSMC-LCB-RM
1	AMSMC-LCB-RP
	Commander, U.S. Army Foreign Science and Technology Center, 220 7th Street, N.E., Charlottesville, VA 22901-5396
3	ATTN: AIFRTC, Applied Technologies Branch, Gerald Schlesinger
	Commander, U.S. Army Aeromedical Research Unit, P.O. Box 577, Fort Rucker, AL 36360
1	ATTN: Technical Library

No. of Copies	To
	Commander, U.S. Army Aviation Systems Command, Aviation Research and Technology Activity, Aviation Applied Technology Directorate, Fort Eustis, VA 23604-5577
1	ATTN: SAVDL-E-MOS
	U.S. Army Aviation Training Library, Fort Rucker, AL 36360
1	ATTN: Building 5906-5907
	Commander, U.S. Army Agency for Aviation Safety, Fort Rucker, AL 36362
1	ATTN: Technical Library
	Commander, USACDC Air Defense Agency, Fort Bliss, TX 79916
1	ATTN: Technical Library
	Commander, Clarke Engineer School Library, 3202 Nebraska Ave., N, Ft. Leonard Wood, MO 65473-5000
1	ATTN: Library
	Commander, U.S. Army Engineer Waterways Experiment Station, P.O. Box 631, Vicksburg, MS 39180
1	ATTN: Research Center Library
	Commandant, U.S. Army Quartermaster School, Fort Lee, VA 23801
1	ATTN: Quartermaster School Library
	Naval Research Laboratory, Washington, DC 20375
1	ATTN: Code 5830
2	Dr. G. R. Yoder - Code 6384
	Chief of Naval Research, Arlington, VA 22217
1	ATTN: Code 471
	Commander, U.S. Air Force Wright Research & Development Center, Wright-Patterson Air Force Base, OH 45433-6523
1	ATTN: WRDC/MLLP, M. Forney, Jr.
1	WRDC/MLBC, Mr. Stanley Schulman
	NASA - Marshall Space Flight Center, MSFC, AL 35812
1	ATTN: Mr. Paul Schuerer/EH01
	U.S. Department of Commerce, National Institute of Standards and Technology, Gaitherburg, MD 20899
1	ATTN: Stephen M. Hsu, Chief, Ceramics Division, Institute for Materials Science and Engineering
1	Committee on Marine Structures, Marine Board, National Research Council, 2101 Constitution Avenue, N.W., Washington, DC 20418
1	Materials Sciences Corporation, Suite 250, 500 Office Center Drive, Fort Washington, PA 19034-3213
1	Charles Stark Draper Laboratory, 68 Albany Street, Cambridge, MA 02139
	Wyman-Gordon Company, Worcester, MA 01601
1	ATTN: Technical Library
	General Dynamics, Convair Aerospace Division P.O. Box 748, Forth Worth, TX 76101
1	ATTN: Mfg. Engineering Technical Library
	Plastics Technical Evaluation Center, PLASTEC, ARDEC Bldg. 355N, Picatinny Arsenal, NJ 07806-5000
1	ATTN: Harry Pebly
1	Department of the Army, Aerostructures Directorate, MS-266, U.S. Army Aviation R&T Activity - AVSCOM, Langley Research Center, Hampton, VA 23665-5225
1	NASA - Langley Research Center, Hampton, VA 23665-5225
1	U.S. Army Propulsion Directorate, NASA Lewis Research Center, 2100 Brookpark Road, Cleveland, OH 44135-3191
1	NASA - Lewis Research Center, 2100 Brookpark Road, Cleveland, OH 44135-3191
	Director, Defense Intelligence Agency, Washington, DC 20340-6053
1	ATTN: ODT-5A (Mr. Frank Jaeger)
	Director, U.S. Army Research Laboratory, Watertown, MA 02172-0001
2	ATTN: AMSRL-OP-CI-D, Technical Library
10	Authors